

# Dissolution of $\gamma'$ Phase in a Single Crystal Superalloy After High-cycle Fatigue

Liu Yuan<sup>1,2</sup>, Wang Linning<sup>1,3</sup>, Yu Jinjiang<sup>1</sup>, Sun Xiaofeng<sup>1</sup>

<sup>1</sup> Institute of Metal Research, Chinese Academy of Sciences, Shenyang 110016, China; <sup>2</sup> Civil Aviation University of China, Tianjin 300300, China; <sup>3</sup> Tianjin University of Technology and Education, Tianjin 300222, China

**Abstract:** High-cycle fatigue (HCF) tests at different temperatures were performed on a single crystal superalloy SRR99 with [001] orientation. The results demonstrate that conditional fatigue strength increases first and then decreases with the increase of temperature, exhibiting the same tendency with tensile strength at elevated temperatures. The microstructures were observed by SEM and TEM and it is found that the morphology of  $\gamma'$  particles changes significantly and dissolution of  $\gamma'$  particles takes place during cyclic loading. This may be induced by the back and forth movement of interface dislocations during the cyclic loading. As a result, the strengthening effect of the coherent  $\gamma/\gamma'$  coherent interfaces is gradually deteriorated during high-cycle fatigue deformation. In addition, the fatigue crack propagation is found to be primarily along a specific crystalline plane, which is identified as (111). The specific mechanism for the microstructure evolution during cyclic loading was discussed based on SEM and TEM observations.

**Key words:** dissolution; precipitation; high-cycle fatigue; single crystal superalloy

Ni-base single crystal superalloys are widely used as turbine blades in aircraft engine due to their superior creep strength at extremely high temperature<sup>[1-8]</sup>. During operation of aircraft engine, turbine blades are subjected to severe vibration and this type of loading can be reasonably evaluated by isothermal high-cycle fatigue tests. Fatigue damage can cause abrupt failure of component and it is very dangerous. Fatigue process is consequence of cyclic plastic deformation and the damage is gradually accumulated in the localized region, which finally causes the rupture of materials<sup>[9-12]</sup>.

The strength of nickel-base superalloy is strongly dependent on the coherent precipitation of  $\gamma'$  phase. Many works on the microstructure of superalloys indicate that the morphology and size of the  $\gamma'$  precipitates play a significant role in high temperature mechanical properties of single crystal superalloy<sup>[13,14]</sup>. After standard solution and aging heat treatment, a large number of cuboidal  $\gamma'$  phases are precipitated in  $\gamma$  matrix and the interface between these two phases is coherent. The coherent interfaces play the most important role in contribution to the strength of Ni-based superalloy at ele-

vated temperatures. In other words, the change of size, morphology and volume fraction of  $\gamma'$  particles will directly deteriorate the high temperature properties. Under condition of applied stress, the motion of dislocations under thermal activation effect increases the interface energy and impairs the stability of  $\gamma'$  phase at high temperature. During creep with the constant applied stress, the primary mechanism for the evolution of  $\gamma'$  phase is the  $\gamma'$  directional coarsening and formation of rafted  $\gamma'$  structure<sup>[15-18]</sup>. However, it is not clear if this mechanism is still dominant under applied cyclic stress at high temperatures.

In the present study, the high-cycle fatigue behavior of a single crystal Ni-based superalloy SRR99 was investigated at different temperatures. First of all, fatigue strength was obtained and compared with high temperature tensile results so as to understand the temperature dependence of fatigue behavior. Second, the microstructures after cyclic deformation were observed by SEM and TEM. The main purpose of this work is to clarify the characteristics of  $\gamma'$  evolution during cyclic loading and to determine the predominant damage mechanism during high-cycle fatigue test.

Received date: September 03, 2019

Corresponding author: Wang Linning, Ph. D., School of Mechanical Engineering, Tianjin University of Technology and Education, Tianjin 300222, P. R. China, Tel: 0086-22-88181083, E-mail: lnwang00@163.com

Copyright © 2020, Northwest Institute for Nonferrous Metal Research. Published by Science Press. All rights reserved.

## 1 Experiment

The material used in this study was a single crystal superalloy SRR99. This alloy is a typical precipitate-strengthened alloy and the volume fraction of  $\gamma'$  particle is 70% approximately. The nominal chemical composition is shown in Table 1.

Single crystal bars with the diameter of 15 mm and length of about 220 mm were produced through directional solidification process. All the alloy bars were cast along [001] direction with deviation no more than  $6^\circ$ . After that, the alloy bars received a standard solution treatment at  $1300^\circ\text{C}$  for 4 h followed by air cooling, and two-step aging treatment at  $1100^\circ\text{C}$  for 4 h and  $870^\circ\text{C}$  for 16 h both followed by air cooling. And then, cylindrical specimens were machined out along [001] direction. The specimen surface was finished with low stress grinding and polishing in order to minimize the influence of surface defects. The specimen geometry is shown in Fig.1.

Fig.2a shows the as-cast microstructure. Due to the presence of segregation of chemical elements during solidification, we can see the dendrite patterns due to the segregation of different chemical elements. After heat treatment, dendrite microstructure vanishes and a large number of  $\gamma'$  particles are embedded in  $\gamma$  matrix, which can be seen in Fig.2b.

All the specimens were fatigue tested under load control at a stress ratio  $R=\sigma_{\min}/\sigma_{\max}=-1$  at a frequency of 83.3 Hz. The tests were conducted at the temperatures of 700, 760, 850 and  $900^\circ\text{C}$ . Rotary bending loading mode was adopted, as a result of sinusoidal waveform performed on the specimens. The specimens for SEM observation were etched by electric polished in a mixture of 8% perchloric acid and ethanol with the etching voltage of 12 V. The thin foils for TEM observation were taken under the fracture surfaces and prepared by twin-jet polishing method.

## 2 Results and Discussion

### 2.1 High-cycle fatigue results

The relationships between stress amplitude and number of cycles to fracture at different temperatures are plotted in Fig.3. It should be noted that the arrows in this figure indi-

**Table 1** Nominal chemical composition of SRR99 alloy (wt%)

Al	Ti	Cr	Co	Ta	W	C	Ni
5.5	2.2	8.5	5.0	2.8	9.5	0.015	Bal.

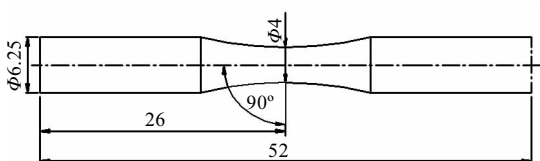


Fig.1 Specimen geometry for high-cycle fatigue test

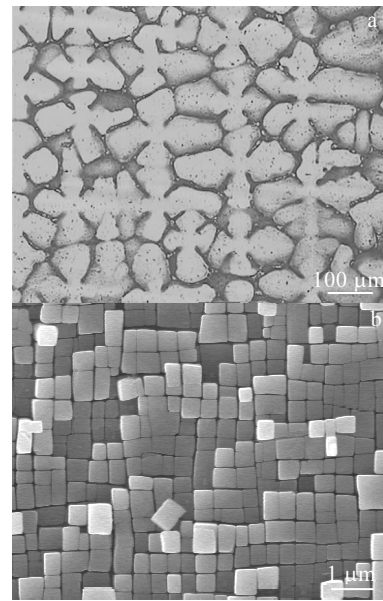


Fig.2 OM image of as-cast dendrite microstructure (a) and SEM image of  $\gamma'$  precipitation (b) in SR99 alloy after heat treatment

cate that these samples do not fail during tests. It is accepted that many factor such as loading mode, stress amplitude and testing temperatures will affect the fatigue life. From this result, we can see the general tendency that the fatigue life decreases with the rise of maximum stress amplitude regardless of the testing temperatures. In addition, the conditional fatigue strength, which is defined as the stress level corresponding to the number of cycles of 107 without failure, is also dependent on testing temperature. The fatigue strength increases first to the maximum value of 365 MPa at  $760^\circ\text{C}$  and then decreases with the increase of temperature. To understand this behavior, we performed tensile tests at the same temperatures because it is believed that the fatigue strength of the material is related with the static tension strength. The results are shown in Table 2. It can be seen that both strengths exhibit the same change tendency with the increase of temperature. As mentioned above, the good high temperature properties of the alloy can be greatly attributed to the  $\gamma'$  strengthening effect. When the temperature increases to a certain value, the strength of  $\gamma'$  by itself will increase [16]. In addition, the absolute value of  $\gamma/\gamma'$  lattice misfit also increases with the increase of temperature. As a result, the motion of dislocations in matrix can be inhibited with higher misfit value and it causes the increase of strength. However, if temperature continues to rise up, the dislocation movement can be facilitated by thermally-assisted cross slip or climb and this will reduce the strength at higher temperatures. In this experiment, the fatigue strength reaching the maximum at  $760^\circ\text{C}$  is likely to be caused, at least in part, by the increased strength of  $\gamma'$  precipitates.

**Table 2 Comparison of fatigue and tensile test results at different temperatures**

Temperature/°C	$\sigma_{0.2}$ /MPa	$\sigma_b$ /MPa	Fatigue strength/MPa
700	990	1160	350
760	1120	1270	365
850	965	1080	350
900	870	1010	335

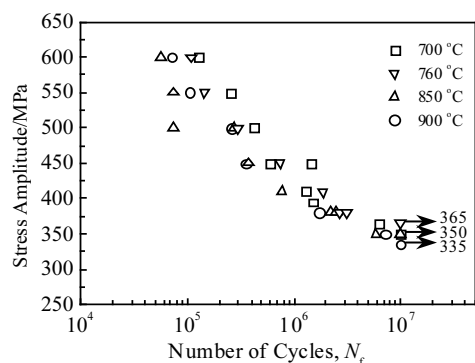


Fig.3 Plot of applied stress amplitude vs number of cycles to rupture at different temperatures (arrows indicate that samples are not tested to failure)

## 2.2 Microstructural examination

As  $\gamma'$  particle is the principal strengthening phase in SRR99 alloy, the cyclic deformation during fatigue loading will bring about the evolution of  $\gamma'$  phase. As can be seen in Fig.4, the morphology of  $\gamma'$  particles changes from cubic to irregular shape. The microstructure of samples tested at different stress levels and temperatures indicates no appreciable differences referring to the  $\gamma'$  morphology and size. This microstructure change is quite different from that during creep deformation, during which  $\gamma'$  rafting takes place. From this result, it is believed that  $\gamma'$  particles during fatigue test dissolve into the matrix channels. It should be noted that even within the same sample, the dissolution process seems not to occur homogeneously because some  $\gamma'$  phases are still cuboidal.

Investigation on the cyclic deformation mechanisms was also conducted through TEM observation, as shown in Fig.5. It can be seen that  $\gamma'$  precipitates lost its original cuboidal shape, which is consistent with the SEM observation. Moreover, these precipitates are surrounded by many interface dislocations. The TEM images shown in Fig.6 indicate that the distribution of dislocations is also quite inhomogeneous. The high density of dislocations is observed in some areas where highly plastic deformation is accumulated. From these observations it can be deduced that the precipitates are surrounded by dislocations and the coherent relationship between  $\gamma/\gamma'$  is lost. The formation of interfacial dislocations can be induced by the interaction between  $\gamma'$  and mobile ma-

trix dislocations<sup>[19]</sup>. With the increase of dislocation density in matrix channel, some dislocations will be trapped by the interfaces. After that, it becomes difficult for mobile dislocations to shear into  $\gamma'$  particles.

## 2.3 Mechanisms for microstructural evolution and fatigue failure

Observation on the microstructure of SRR99 alloy after cyclic loading at elevated temperatures indicates that significant changes of  $\gamma'$  morphology occur due to the cyclic plastic deformation. The presence of cyclic stress and the

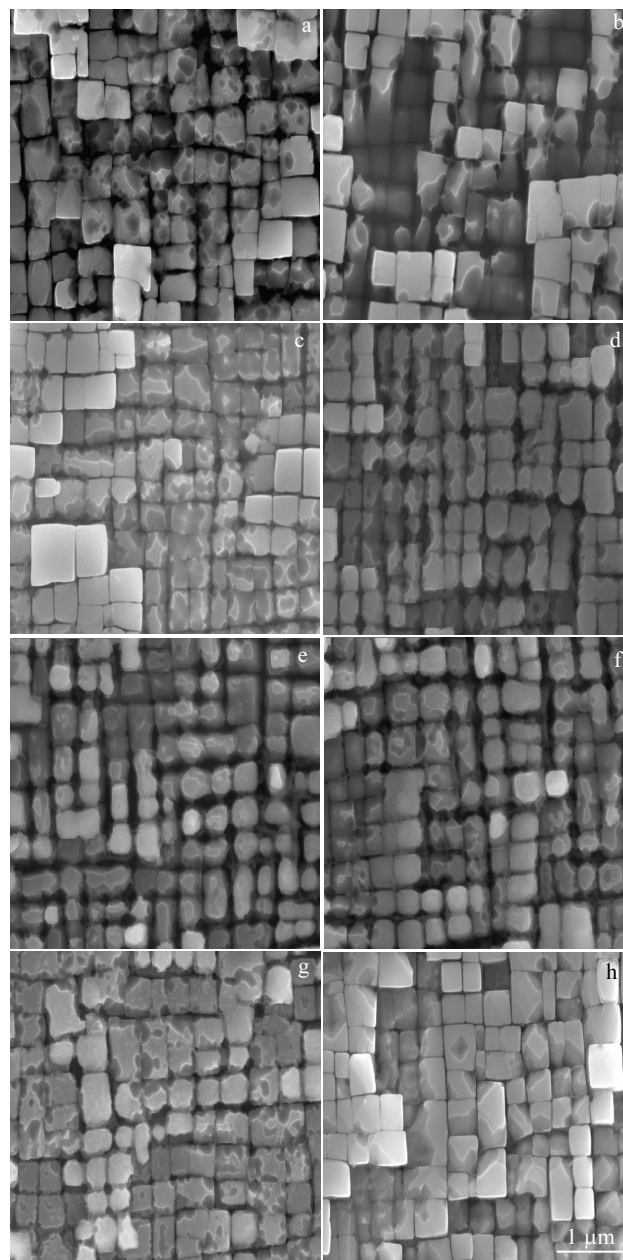


Fig.4 SEM images of microstructure after cyclic deformation tested at different temperatures and loads: (a) 700 °C, 500 MPa; (b) 700 °C, 365 MPa; (c) 760 °C, 500 MPa; (d) 760 °C, 380 MPa; (e) 850 °C, 500 MPa; (f) 850 °C, 350 MPa; (g) 900 °C, 500 MPa; (h) 900 °C, 350 MPa

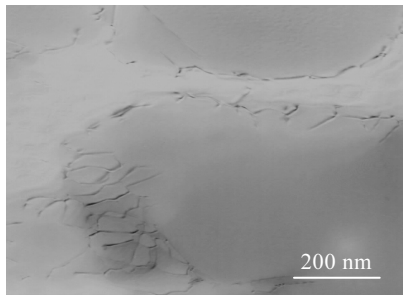


Fig.5 TEM image of interfacial dislocation configuration at 700 °C/600 MPa

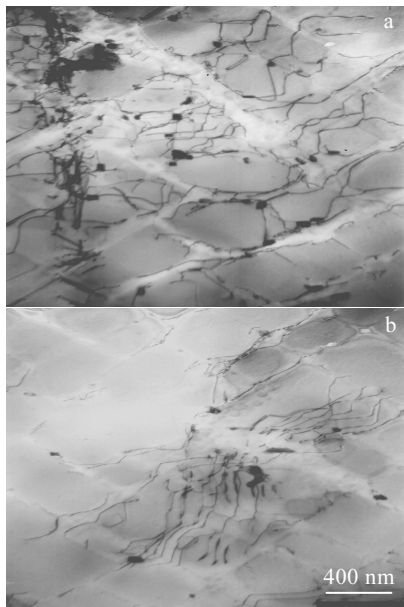


Fig.6 TEM images of distribution of dislocations after fatigue test at 760 °C, 365 MPa (a) and 760 °C, 600 MPa (b)

resultant plastic deformation induce the dissolution of  $\gamma'$ , but no rafted microstructure is observed in SRR99 alloy after high-cycle fatigue tests, which is quite different from the microstructure evolution during creep. It can be deduced that  $\gamma'$  dissolution within all the specimens is induced by the interaction of cyclic plastic deformation and high temperature.

Morphology instability is related to both diffusion of chemical elements and other factors like surface energy, anisotropy of surface tension<sup>[2]</sup>. After optimized heat treatment, the  $\gamma'$  particles are completely embedded in the matrix channel and coherent with the  $\gamma$  phases. Both the coherent strain and the interface energy in cuboidal  $\gamma'$  are at a low stage. The matrix of SRR99 alloy is facet-centered cubic structure and the easy-slipping systems are identified as  $\{111\} \langle 110 \rangle$ . It is reported that matrix dislocation type can be identified as  $[110]$  on  $(111)$  planes<sup>[5,16,20]</sup>. When the samples are subjected to cyclic stress at elevated temperatures, a large number of dislocations are generated on the  $(111)$  planes of matrix channels. Thereafter, the to and fro motion of these dislocations

will be trapped by the  $\gamma/\gamma'$  interface and the coherent interface gradually changes to be non-coherent. This process generally takes place during mechanical test as long as the temperature is high enough and the duration is long enough to move dislocations from the resources. The formation of interface dislocations is schematically shown in Fig.7. As a consequence, the surface energy of  $\gamma'$  particles will increase and the lattice misfit is altered by the increased density of interface dislocations. With the accumulation of cyclic plastic deformation, the interface energy is increased, which means that the activation energy required for element diffusion is reduced<sup>[21]</sup>. In order to maintain the low surface energy, some elements commence to dissolve into the matrix and induce the significant change of cuboidal  $\gamma'$  morphology.

The change in  $\gamma'$  morphology plays an important role in the high temperature properties of the alloy. One of the direct outcomes brought about by  $\gamma'$  dissolution is the widening of matrix channels. With the increase of the channel width, the back and forth motion of matrix dislocations is facilitated and the formation of slip bands is subsequently accelerated. It is reported that at low and medium temperatures, the strength of the alloy is determined by the width of the matrix channels<sup>[16]</sup>. For another, the coherent strain field generated by  $\gamma/\gamma'$  misfit is deteriorated during the process of dissolution of  $\gamma'$  particles, and then strengthening effect of  $\gamma'$  is impaired. With the accumulation of plastic deformation, slip bands are generally found in the samples after cyclic deformation and these bands will provide preferential sites for small crack nucleation. Fig.8 illustrates a typical fractograph after high-cycle fatigue. It should be noted that most fracture surfaces demonstrate a cleavage fracture feature. And then we cut the sample along the longitudinal direction to observe the crack propagation behavior. It is worth noting that the crack seems to be straight and propagates along a specific crystal plane. Since all the samples used in this study are  $[001]$  crystals. The angle between the crack traces and axial direction is approximately  $54^\circ$ , which is quite close to the angle between  $[001]$  and  $[111]$  crystal direction. Therefore it can be determined that the fatigue crack primarily propagates on  $(111)$  crystalline plane. The predominant mechanism for SRR99 alloy after high-cycle fatigue failure can be proposed as follows: cyclic loading induces the formation of interface dislocations; these dislocations will lead to the change of  $\gamma'$

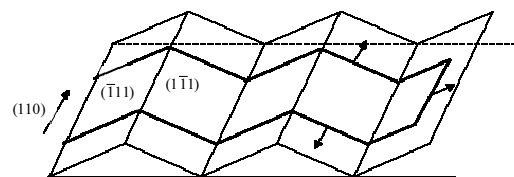


Fig.7 Schematic illustration of the dislocation motion in matrix channels

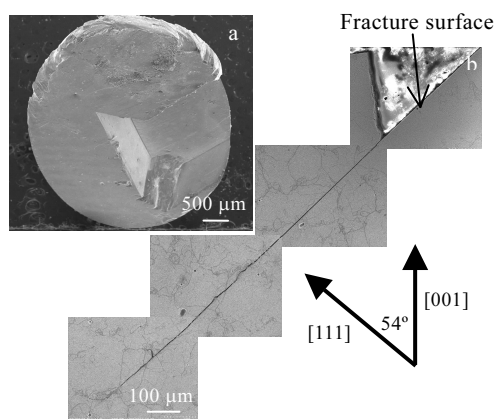


Fig.8 Fracture surface after high-cycle fatigue test at 760 °C with the stress amplitude of 450 MPa (a) and fatigue crack propagation in the same sample (b)

morphology; as a consequence, the strengthening effect from  $\gamma/\gamma'$  coherent interface significantly deteriorates. This process promotes the formation of slip bands and subsequently enhances the nucleation and propagation of fatigue cracks on (111) crystalline plane.

### 3 Conclusions

1) The fatigue strength is dependent on the testing temperature and the peak value is found at 760 °C, showing a good agreement with the variation of tensile strength at elevated temperatures.

2) After fatigue deformation, the morphology of  $\gamma'$  precipitates significantly changes and the dissolution of  $\gamma'$  precipitates occurs regardless of the loading temperature and applied cyclic stress levels. This phenomenon can be attribute to the interaction between dislocations and  $\gamma/\gamma'$  coherent interfaces. With the dissolution of  $\gamma'$  particles, the strengthening effect of  $\gamma'$  is substantially deteriorated. Resultantly, the fatigue crack nucleates and propagates along a specific crystalline plane.

### References

- Cormier J, Milhet X, Mendez J. *Acta Materialia*[J], 2007, 55: 6250
- Yoo Y S. *Scripta Materialia*[J], 2005, 53: 81
- Steuer S, Hervier Z, Thabart S et al. *Materials Science and Engineering A*[J], 2014, 601: 145
- Giraud R, Hervier Z, Cormier J et al. *Metallurgical and Materials Transaction A*[J], 2012, 43: 3988
- Ram F, Li Z, Zaefferer S et al. *Acta Materialia*[J], 2016, 109: 151
- Zhang J X, Murakumo T, Kobayashi T et al. *Acta Materialia*[J], 2003, 51: 5073
- Pollock T M, Argon A S. *Acta Metallurgica et Materialia*[J], 1994, 42: 1859
- Yue Q, Liu L, Yang W et al. *Materials Science and Engineering A*[J], 2019, 742: 132
- Chen J, Cao L, Xue M et al. *Rare Metals*[J], 2014, 32(2): 144
- Mukherji D, Piegert S, Rosler J. *Material Science Forum*[J], 2003, 426: 815
- Yang X, Dong C, Shi D et al. *Materials Science and Engineering A*[J], 2011, 528(22): 7005
- Huang M, Cheng Z, Xiong J et al. *Acta Materialia*[J], 2014, 76: 294
- Acharya M V, Fuchs G E. *Scripta Materialia*[J], 2006, 54: 61
- Grosdidier T, Hazotte A, Simon A. *Scripta Metallurgica et Materialia*[J], 1994, 30: 1257
- Yue X, Li J, Wang X. *Rare Metals*[J], 2018, 37(3): 210
- Feller-Kniepmeier M, Link T, Poschmann I. *Acta Materialia*[J], 1996, 44: 2397
- Nabarro F R N. *Metallurgical and Materials Transaction A*[J], 1996, 27: 513
- Costa A, Hawk E, Dansbury J. *Journal of Materials Engineering and Performance*[J], 2018, 27(11): 5744
- Hwang S K, Lee H N, Yoon B H. *Metallurgical and Materials Transaction A*[J], 1989, 20: 2793
- Shui L, Xu Y, Hu Z. *Rare Metal Materials and Engineering*[J], 2018, 47(4): 1054
- Nategh S, Sajjadi S A. *Materials Science and Engineering A*[J], 2003, 339: 103

## 一种镍基单晶高温合金高周疲劳引起的 $\gamma$ 溶解行为

刘源<sup>1,2</sup>, 王琳宁<sup>1,3</sup>, 于金江<sup>1</sup>, 孙晓峰<sup>1</sup>

(1. 中国科学院金属研究所, 辽宁 沈阳 110016)

(2. 中国民航大学, 天津 300300)

(3. 天津职业技术师范大学, 天津 300222)

**摘要:** 研究了一种镍基单晶高温合金 SRR99 在不同温度下的高周疲劳行为, 试样采用[001]取向的单晶棒。结果表明, 条件疲劳强度随着试验温度的升高先上升后降低, 与高温拉伸强度表现出相同的变化规律。通过扫描电子显微镜和透射电子显微镜的观察发现 $\gamma$ 相的形貌发生了显著变化, 经过高温循环变形后 $\gamma$ 析出相发生了溶解。在交变应力的作用下,  $\gamma$ 与基体界面产生大量的位错, 而位错的往复运动引起了 $\gamma$ 相的溶解。因此循环加载过程中伴随着 $\gamma$ 的不断溶解, 共格界面的强化作用不断减弱。除此之外, 通过裂纹扩展方向与试样轴向的夹角可以判断出疲劳裂纹的扩展主要沿着(111)晶面进行。根据扫描电镜和透射电镜的观察结果, 对循环加载的微观组织演化机理进行了讨论。

**关键词:** 溶解; 析出相; 高周疲劳; 单晶高温合金

**作者简介:** 刘源, 男, 1981年生, 博士, 中国民航大学航空工程学院, 天津 300300, 电话: 022-24092404, E-mail: Ivan\_liu1026@hotmail.com